


Article

Green Composites Based on PLA and Cotton Fabric Waste: Preparation and Characterization

Narongchai O-Charoen¹, Piyaporn Kampeerapappun², Khanittha Charoenlarp², Nawadon Petchwattana³ and Ektinai Jansri^{4,*} 

¹ Department of Materials and Metallurgical Engineering, Faculty of Engineering, Rajamangala University of Technology Thanyaburi, Pathumthani 12110, Thailand

² Faculty of Textile Industry, Rajamangala University of Technology Krungthep, Bangkok 10120, Thailand

³ Department of Chemical Engineering, Faculty of Engineering, Srinakharinwirot University, Nakhon Nayok 26120, Thailand

⁴ Division of Polymer Materials Technology, Faculty of Agricultural Product Innovation and Technology, Srinakharinwirot University, Nakhon Nayok 26120, Thailand

* Correspondence: ektinai@g.swu.ac.th

Abstract: Textile waste, from both consumption and production, has dramatically increased due to a lack of diversification in its use. Increasing the number of textile alternatives can help to solve these problems. Producing a green composite product is an interesting alternative method. The objectives of this work were to study the preparation and characterization of green composites created from PLA and cotton fabric waste (CFW) and to consider the effect of the CFW content on the composites. The procedure of the research began with CFW pellets preparation; this was subsequently compounded with PLA pellets using a melt-mixing technique with a twin-screw extruder at ratios of 90:10, 80:20, and 70:30 wt% between the PLA and cotton fabric waste, respectively. Then, the testing specimens were produced by compression molding. The experiments demonstrated that an increase in the CFW caused an increase in the viscosity, stiffness, T_g , T_m , and water absorption of the composites. The decomposition temperature of the composites showed a range of 302.41 to 361.22 °C; this decreased when the CFW increased. An increase in the CFW also produced greater and clearer phase separation and roughness on the fracture surface area.

Keywords: green composites; cotton; fabric waste; polylactic acid; textile recycling



Citation: O-Charoen, N.; Kampeerapappun, P.; Charoenlarp, K.; Petchwattana, N.; Jansri, E. Green Composites Based on PLA and Cotton Fabric Waste: Preparation and Characterization. *Recycling* **2022**, *7*, 78. <https://doi.org/10.3390/recycling7050078>

Academic Editor: Francesco Paolo La Mantia

Received: 28 August 2022

Accepted: 17 October 2022

Published: 19 October 2022

Publisher's Note: MDPI stays neutral with regard to jurisdictional claims in published maps and institutional affiliations.



Copyright: © 2022 by the authors. Licensee MDPI, Basel, Switzerland. This article is an open access article distributed under the terms and conditions of the Creative Commons Attribution (CC BY) license (<https://creativecommons.org/licenses/by/4.0/>).

1. Introduction

Currently, PLA is the most widely used biodegradable polymer. It is used in the medical, automotive, textile, food, and agricultural industries because it has appropriate mechanical properties and transparency. It can also be molded in various processes. However, it has also disadvantages, such as a low operating temperature and brittleness. It is also relatively expensive. Improving the properties of PLA can be achieved by adding thermal stabilizers such as carbon powder, titanium dioxide, or titanium dioxide nanoparticles [1–6] or reinforcing materials such as glass fiber, natural fibers, or charcoal powder to provide greater strength and flexibility [7–9]. Production costs can be reduced by adding cassava starch [10,11]. Improving strength by reinforcing biodegradable natural materials combined with a PLA matrix can be termed a “green composite material” because both are biodegradable materials [12,13].

Cotton fiber is the natural fiber most commonly used in the textile industry because of its many notable properties such as high tensile strength and easy processing. It can be mixed with other fibers to easily create the characteristics of yarn. Cotton fibers are mostly used for garments, but they are also used for other applications such as reinforcement in polymers [14].

Recently, technology has changed, as has the lifestyle of people as a result of rapid population growth. Clothing manufacturers have adapted to these changes by increasing mass production, reducing product quality, and producing disposable clothing. All of these factors cause “fast fashion”, dramatically increasing clothing waste in a short time as well as the waste from the upstream production process such as fabric and yarn waste. Most waste management methods usually use a landfill site [15]. In a few countries with limited space, waste is sent to be buried in other areas; this causes the costs to increase. Therefore, the use of fabric waste for other applications may be more cost-effective than conventional waste management methods. The use of waste fabric as a reinforcement for polymers is one method that can help to reduce waste problems and also, improve the properties of polymers [16–18].

Several studies have examined the use of natural fibers to reinforce PLA. The modulus of PLA increased up to 50% when 30% natural fibers were used with epoxidized jatropa oil [19]. The cellulose extracted from natural fibers could increase the PLA strength to a maximum of 60% [20]. In the case of PLA reinforced with cotton fibers, it was observed that using cotton gin waste (CGW) obtained from the by-products of the gin-making process could increase the flexural modulus of PLA by 42% with a 30% CGW addition [21]. The yield stress of PLA increased by 30% when it was mixed with waste cotton fibers [22]. The mixing of cotton waste derived from waste garments with PLA at various ratios from 2–15%, together with a PP-g-MA of 5%, had higher tensile strength than pure PLA in all cases [23]. The use of absorbent cotton fibers as a reinforcement to PLA can be achieved by cutting the fiber to a shorter length and a certain length. After that, mixed with PLA and a coupling agent by the torque rheometer, and produced the samples by injection molding. Such a composite preparation method will allow higher tensile strength, impact strength, and flexural modulus than PLA pure in all cases. However, it should be noted that if the cotton fiber content is more than 20%, the tensile and impact strength tended to decrease [24]. Past research has demonstrated that too great a focus has been placed on using cotton pure (unprocessed textiles) and recycling clothing waste. Another point has also been overlooked: the volume of waste from garment production factories is also difficult to manage.

Therefore, in this paper, we researched the preparation and characterization of green composites from PLA and cotton fabric waste (CFW). We used a simple technique to change the CFW fiber to CFW pellets by compression molding and a die-cut machine. Then the twin screw extruder was used compounding to produce the green composite of PLA and CFW at the ratio of 90:10, 80:20, and 70:30 wt%. The molded specimens were then tested by compression molding. Finally, the mechanical properties, fractured morphology, thermal properties, and water absorption of the composites were investigated.

2. Results and Discussion

2.1. CFW Pellets Characterization

The CFW appearance is shown in Figure 1. The dimensions of the CFW pellets had an average length of 2.73 ± 0.28 mm, an average width of 1.67 ± 0.22 mm, and an average thickness of 0.21 ± 0.13 mm. The density was equal to ~ 1.40 g/cm³.

2.2. Melt Flow Index

As expected, the results clearly showed that the CWF interfered with the movement of the PLA molecular chains, causing the melt flow rate of the PLA to decrease with an increase in the CWF content, as shown in Table 1.



Figure 1. CFW pellets.

Table 1. The melt flow index.

| Samples | Melt Flow Rate (g/10 min) 210 °C/2.16 kg |
|---------|--|
| PLA | 6.19 ± 0.20 |
| CFW10 | 5.37 ± 0.08 |
| CFW20 | 3.98 ± 0.21 |
| CFW30 | 1.91 ± 0.05 |

2.3. Mechanical Properties

Figure 2 shows the graph of the tensile strength and tensile modulus testing. The results showed that the tensile strength of the pure PLA was the highest at 58.4 MPa, followed by CFW10, CFW20, and CFW30 at 25.8, 20.3, and 17.5 MPa, respectively. These were directly the result of the immiscibility and poor interaction of the PLA and CFW, which caused a dramatic phase separation when the CFW content increased. In contrast, the tensile modulus of CFW30 was the highest at 23.3 GPa, followed by CFW20, CFW10, and pure PLA at 20.2, 12.4, and 5.62 Gpa, respectively. The results of the tensile modulus clearly showed that adding CFW pellets into PLA could help to improve the stiffness.

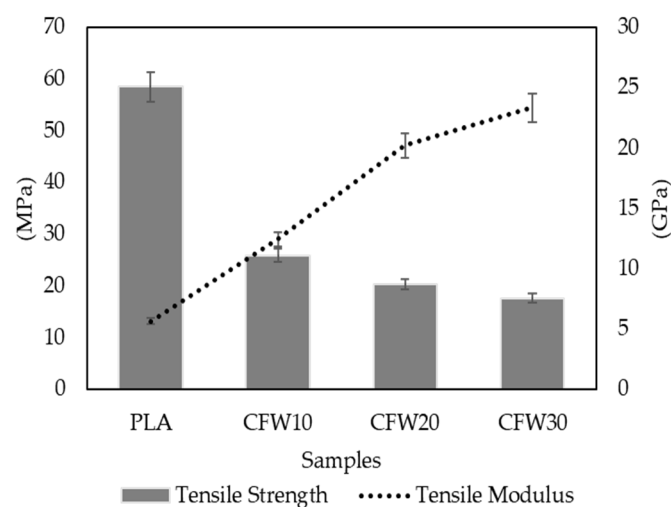


Figure 2. Tensile strength and tensile modulus of PLA/CFW.

The graph of the flexural strength testing is shown in Figure 3. The results showed that CFW30 had the highest flexural strength at 15.7 MPa, followed by pure PLA, CFW20, and CFW10 at 14.2, 9.7, and 8.2 MPa, respectively. It should be noted that the cases of CFW10 and CFW20 had a lower flexural strength than PLA pure. This may be the result

of the poor distribution of the fibers in the matrix, resulting in a low continuation phase, especially in CFW10. While CFW30 showed a higher continuation phase due to the fibers distributed evenly in the matrix. Figure 4 shows the appearance of PLA/CFW from the optical microscope. In the case of CFW10, the CFW pellets had loosened slightly due to low shear causing the formation of a loosely distributed CFW pellet in the PLA matrix, the specimen had a high light transmittance (low continuation phase). In the cases of CFW20 and CFW30, the CFW pellets had more loosened and became fine fibers due to higher shear causing the specimens had low light transmittance (high continuation phase) for CFW20 and opaque for CFW30, respectively. Moreover, it may include a result of the favorable entanglement of a polymer chain with filler which has overcome the weak filler matrix adhesion. As a result, the flexural strength increased [25,26].

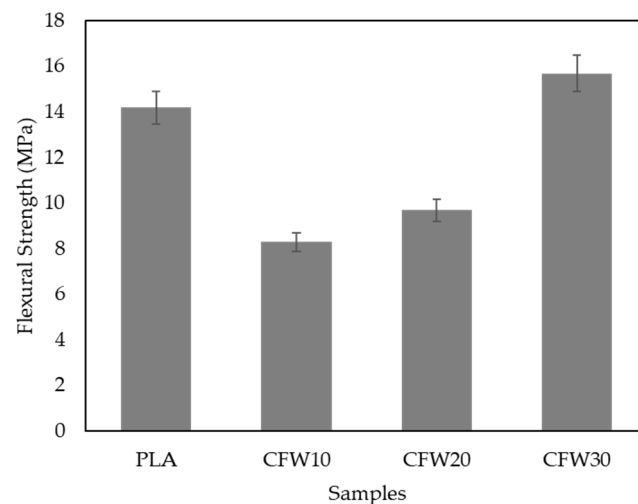


Figure 3. Flexural strength of PLA/CFW.

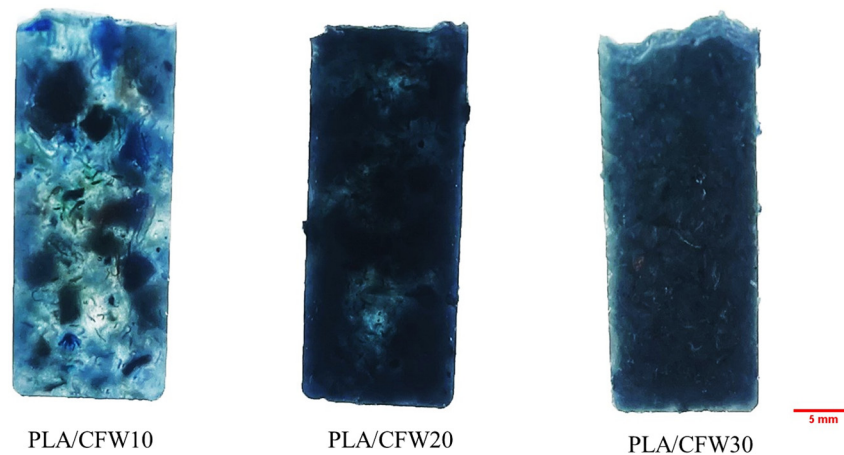


Figure 4. The appearance of PLA/CFW.

The Izod impact strength testing is shown in Figure 5. The result was similar to the flexural strength; CFW30 was the highest at 5.51 kJ/m^2 , followed by pure PLA, CFW20, and CFW10 at 2.60 , 2.51 , and 1.50 kJ/m^2 , respectively. The result indicates that the CFW was able to absorb energy because of the encouraging entanglement of fiber and matrix. This is related to the fiber pull-out, an important energy dissipation mechanism in composites reinforced with fiber. The increase in CFW content causes requires a higher force to pull out the fiber. As a result, the impact strength increased [25,26]. Figure 6 shows fiber distribution on the fracture surface from Izod impact strength specimens. It can be seen that the fiber concentration increases with increasing CFW content.

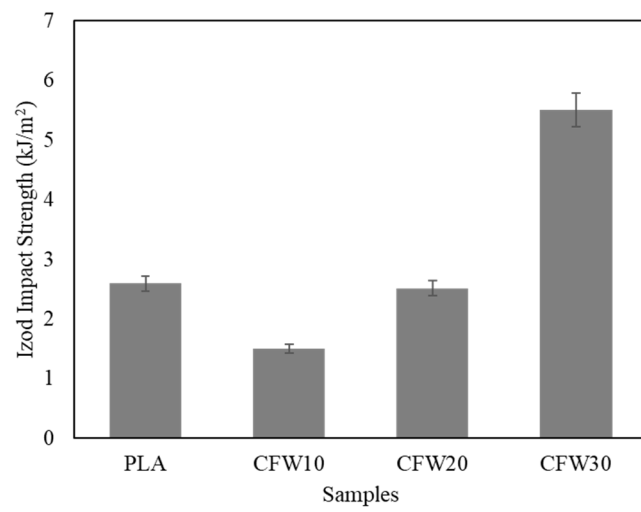


Figure 5. Izod impact strength of PLA/CFW.

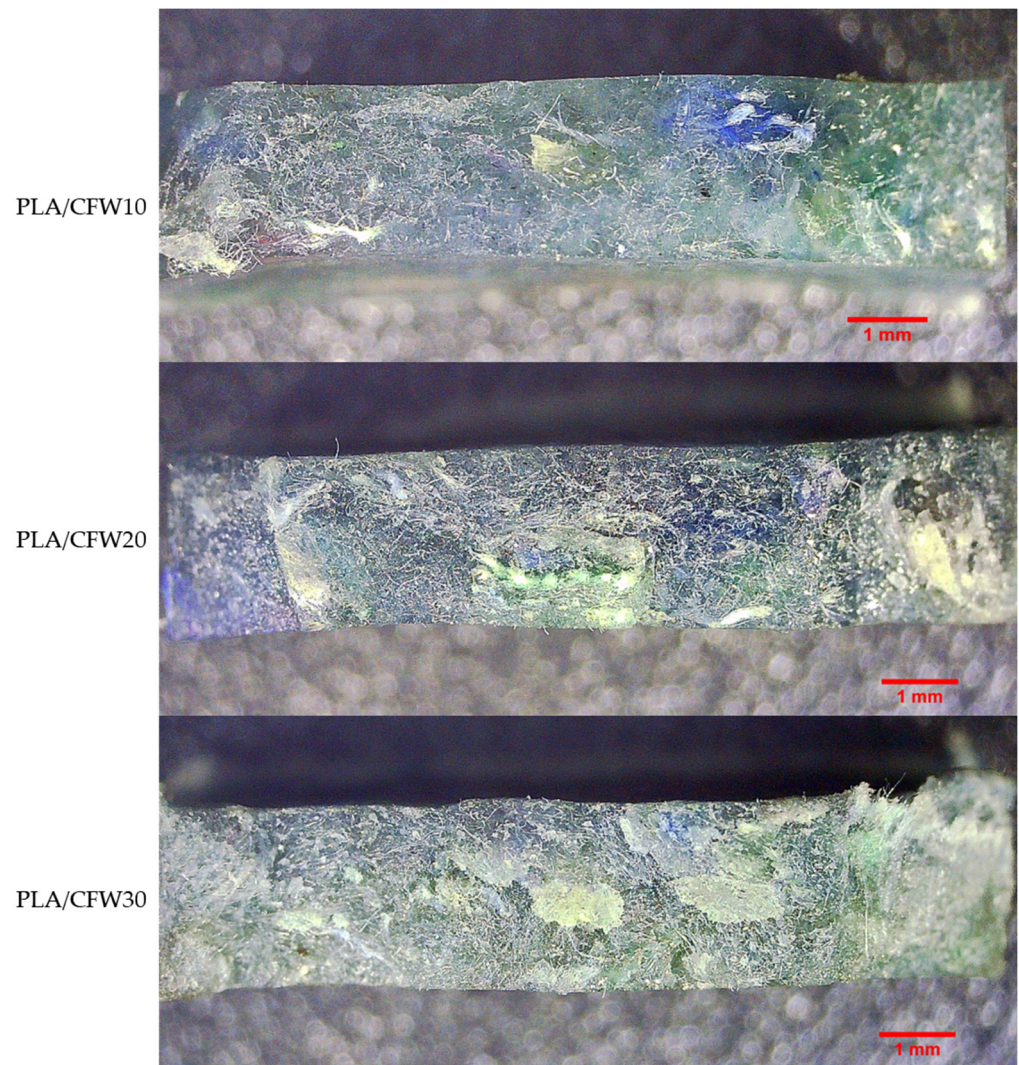


Figure 6. Fiber distribution on the fracture surface.

2.4. Fracture Morphology

Figure 7 shows the fracture pictures of the PLA/CFW composites with varying CFW contents obtained by a digital microscope. We observed that pure PLA had a smooth and

sharp fracture surface. In the case of the composites, phase separation clearly occurred when the CFW content increased; they had a rough fracture surface that indicated an immiscible blend of PLA and CFW. With low CFW content, the fibers were aggregated, clumped, and had an unregular distribution. With higher CFW content, and with greater friction in the compounding step, the fibers were regularly distributed in the PLA matrix. An increase in the phase separation may have resulted in the microstructure of the specimens having a greater number of stress concentration points; this could have resulted in a decrease in the mechanical properties when force was applied to the subject. The image analysis processing used to measure the roughness is shown in Figure 7 (analyzed image); low and high color contrasts represent the smooth and rough surfaces, respectively. The results in terms of numerical corresponded with the visual observation. An increase in the CFW content resulted in greater roughness, as shown in Table 2.

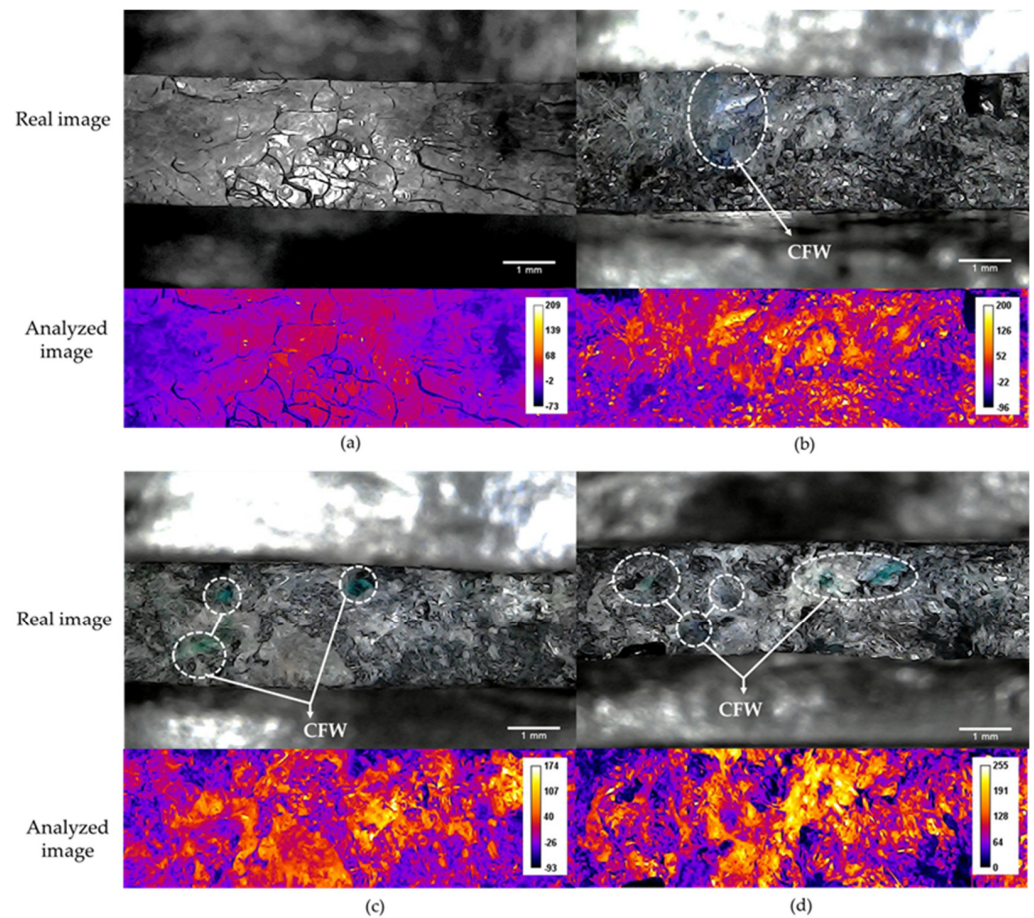


Figure 7. Fracture morphology and roughness analysis of materials: (a) PLA; (b) PLA/CFW10; (c) PLA/CFW20; (d) PLA/CFW30.

Table 2. Arithmetic means surface roughness of the fracture.

| Samples | Arithmetic Means Of Surface Roughness, Ra (Micron) |
|---------|--|
| PLA | 16.02 |
| CFW10 | 34.11 |
| CFW20 | 40.47 |
| CFW30 | 52.53 |

2.5. Thermal Properties

Figure 8 shows the DSC thermograms, indicating the melting temperature (T_m) and the glass transition temperature (T_g) of the pure PLA and PLA/CFW composites. As expected,

the graphs indicated only one endothermic peak appearing for the second heating of all the cases, in which the value was close to pure PLA. It can be assumed that some polymeric compounds that may remain from the finishing and dyeing of CFW did not affect the melting temperature of PLA. The thermal properties are summarized in Table 3. We observed that the T_g increased with an increase in the CFW content because the CFW hindered the mobility of the polymer chain. This was one of the reasons that the rigidity of the composites increased. [27]. The T_m was slightly increased because CFW can affect the factor of crystallization, molecular weight, chain branching, or cross-linking [28]. The crystallinity percentage showed that the CFW could induce PLA to crystallization [29], whereas an increase in the CFW content did not have a significant effect.

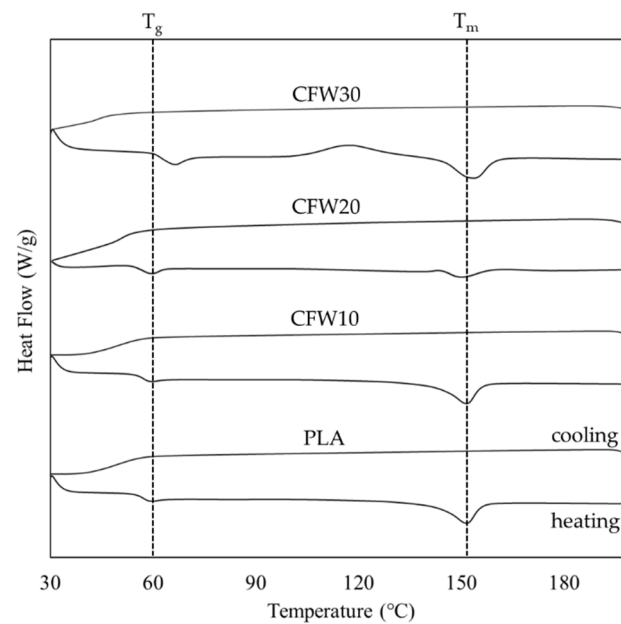


Figure 8. DSC thermograms.

Table 3. Thermal property data of the PLA/CFW composites.

| Samples | Differential Scanning Calorimetry (DSC) | | | Thermogravimetric Analysis (TGA) | | |
|---------|---|------------|--------------------------|----------------------------------|--|---|
| | T_g (°C) | T_m (°C) | Crystallinity (% X_c) | Weight Loss (%) | Temperature Decomposition (T_{onset}) (°C) | Temperature Decomposition (T_{peak}) (°C) |
| PLA | 58.87 | 148.61 | 1.09 | 98.93 | 333.56 | 372.12 |
| CFW | - | - | - | 87.88 | 314.75 | 431.75 |
| CFW10 | 61.11 | 150.03 | 3.56 | 93.85 | 315.24 | 361.22 |
| CFW20 | 63.52 | 152.91 | 1.73 | 93.83 | 306.98 | 359.10 |
| CFW30 | 66.31 | 153.54 | 1.68 | 93.07 | 302.41 | 356.57 |

The relationship between the weight loss and an increase in the temperature of the composites was measured by a TGA. As shown in Figure 9, both PLA and PLA/CFW showed degradation in a single step at temperatures ranging from 333.56 to 372.12 °C and 302.41 to 361.22 °C, respectively. Whereas, CFW showed degradation in the double step as shown in Figure 9b. The first step, the temperature range of 321.72–348.89 °C, correlates to cellulose dehydration and decarboxylation reactions, which result in combustible gasses. The second step, the temperature range of 404.47–436.73 °C, can be attributed to the oxidative degradation of the char formed in the first step [30,31]. Thus, the presence of CFW in the PLA matrix resulted in a decrease in the thermal stability of the composites.

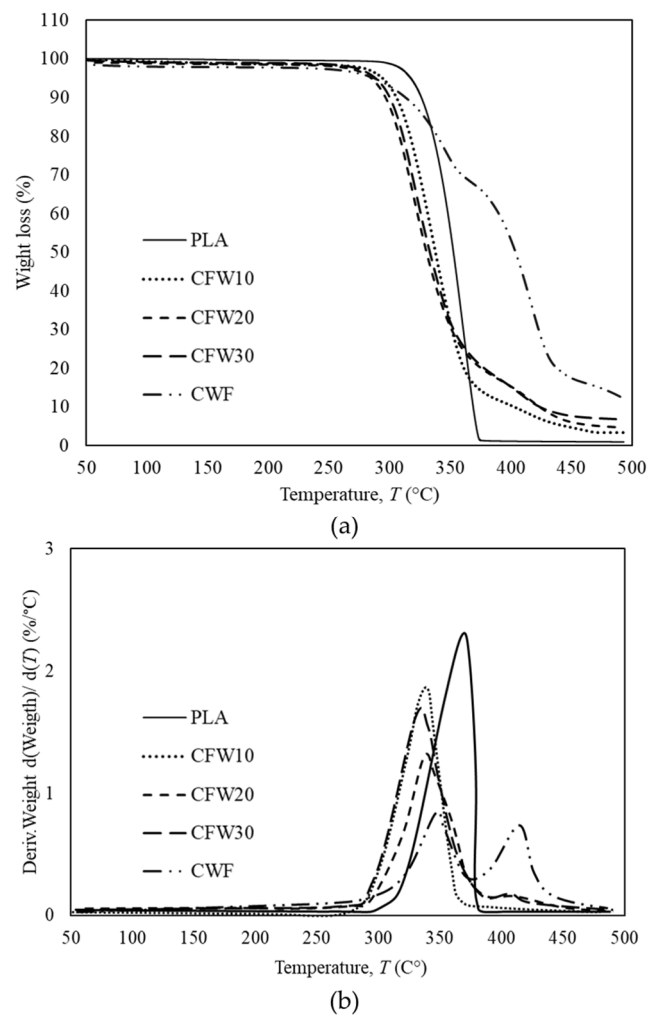


Figure 9. (a) TGA and (b) DTG thermograms of the PLA/CFW.

2.6. Water Absorption

Figure 10 shows the water absorption percentages of the pure PLA and PLA/CFW composites. CFW30 had the highest water absorption percentage, followed by CFW20, CFW10, and PLA at 8.76, 7.16, 1.77, and 0.34%, respectively. This was likely the result of an increase in the hydroxyl groups, which are hydrophilic functional groups [23].

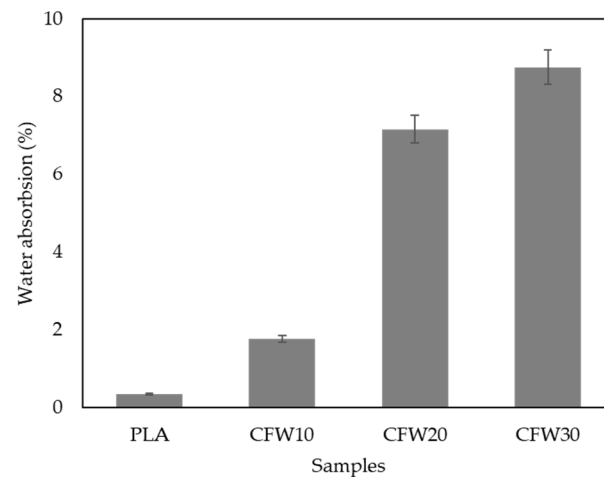


Figure 10. Water absorption.

3. Materials and Methods

3.1. Materials

We used polylactic acid (PLA), grade 2003D (NatureWorks LLC product, Plymouth, MN, USA), obtained from PTT Global Chemical PCL (Bangkok, Thailand) with a melt flow rate of 6.00 g/10 min at 210 °C/2.16 kg, a melting temperature of 210 °C, and specific gravity of 1.21. A PLA sheet, grade 2003D, with a thickness of 0.3 mm was obtained from Thai Materials Development Co., Ltd. (Uthaitani, Thailand). The cotton fabric waste (CFW) was obtained from Ratana Apparel Cares Co., Ltd. (Nontaburi, Thailand) and was treated and dyed with typical finishing agents.

3.2. Method

The CFW had undergone transformation processing from fabric to fibers, which caused the fibers to be fluffy and tangled. It was difficult to define the characteristics or quality. Therefore, it could not be directly mixed with PLA by a twin-screw extruder. Thus, the CFW had to be prepared in an appropriate form, which were CFW pellets. The preparation of the CFW pellets was achieved as follows: the CFW was placed in the middle of a PLA film in a sandwich structure and laid down on a mold with a thickness of 2 mm. The mass of the PLA sheet and CFW were 30 and 60 g. In the second step, a compression molding machine was used at a temperature of 190 °C with a compression time and cooling time of 3 min each (total of 6 min). We then obtained a CFW sheet. In the third step, a die-cutting machine was used to cut the CFW sheet to form the CFW pellets. The procedure of the CFW pellets preparation is shown in Figure 11.

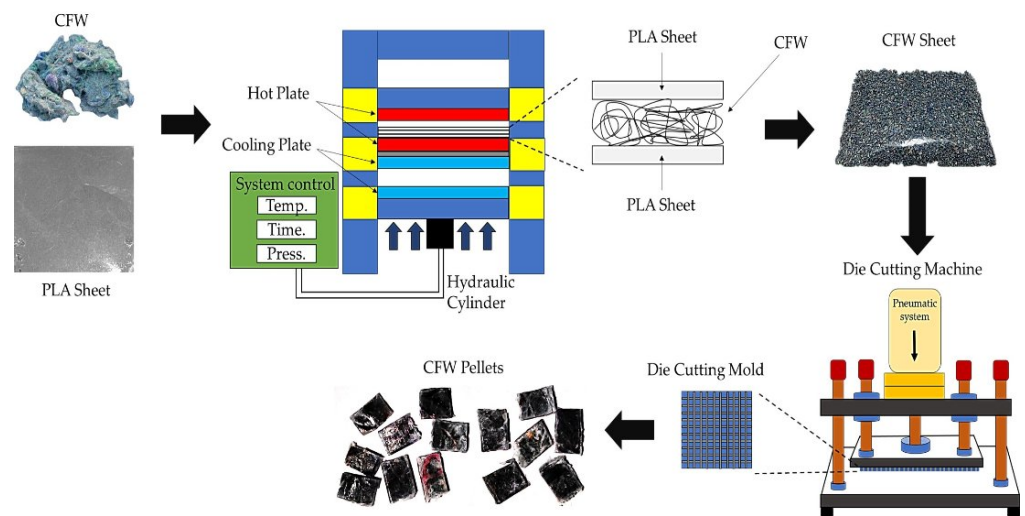


Figure 11. Schematic of the CFW pellet preparation.

The PLA/CFW composite preparation began with the elimination of the moisture in the pellets using an oven at 80 °C for 5 h. The PLA and CFW pellets were then mixed by dry blending technique at ratios of 90:10, 80:20, and 70:30 wt% in rotary drum tumbler mixers for 10 min, then mixed again by melt blending technique with a twin-screw extruder at an approximate temperature of 130–170 °C and screw speed of 60 rpm. Finally, the PLA/CFW pellets were molded by a compression molding machine at a temperature of 190 °C and a compression time and cooling time of 5 minutes each (total of 10 min) to obtain the test specimens. The composites with various CFW pellets ratios were identified as CFW10 for the 90:10 ratio, CFW20 for the 80:20 ratio, and CFW30 for the 70:30 ratio.

3.3. Characterization

3.3.1. CFW Pellets Characterization

The purpose of this measurement is to identify the characteristics of the CFW pellets after preparation. The CFW pellets were observed with a digital microscope with

a maximum magnification of 600× and then analyzed by using the ImageJ software to measure the average width, length, and thickness. The density was investigated by an electronic densimeter.

3.3.2. Melt Flow Test

The melt flow index (MFI) test was used to investigate the rheology of the PLA/CFW composites. The data from the test were reported as the weight (g) per 10 min. A melt flow index machine from C.B.N. Material test Co., Ltd. (Bangkok, Thailand), model XRL-400A, was used. The testing condition was set according to ASTM D1238 at a temperature of 210 °C and a load of 2.16 kg.

3.3.3. Mechanical Properties

The mechanical properties of the PLA/CFW composites were tested for tensile, flexural, and Izod impact strength. The tensile strength was tested according to ASTM D638 by a universal testing machine (Instron, model 3400) with a cross-head speed of 50 mm/min. The results were reported in terms of the tensile strength (MPa) and tensile modulus (GPa). The flexural strength was tested according to ASTM D790 in a machine similar to the tensile test with a cross-head speed of 2 mm/min. The results were reported in terms of flexural strength (MPa). The Izod impact strength was tested according to ASTM D256 using a CEST model 6542 Serial 833. The results were reported in terms of the impact strength (kJ/m²).

3.3.4. Fracture Morphology

A digital microscope was used to investigate the fibers embedded within the PLA matrix. An increase in the fiber content in the specimens would result in individual images being different in terms of surface smoothness. Therefore, ImageJ software was used for the analysis in terms of the arithmetic means of the surface roughness, Ra (micron), using the SurfCharJ function [32].

3.3.5. Thermal Properties

A melting temperature transition (T_m), a glass temperature transition (T_g), and a crystallinity ($\%X_c$) temperature transition (T_c) were investigated using differential scanning calorimetry (DSC). DSC was performed using a NETZSCH, model DSC 200 F3, with a heating rate of 10 °C/min from 30 °C to 200 °C, which was then held for 5 minutes to remove the thermal history, then the heat was reduced by 10 °C/min from 200 °C to 30 °C and heated again in a similar to the first heating condition. The following equation was used to compute the crystallinity of the composites:

$$X_c(\%) = \frac{\Delta H}{\Delta H_{f(100)}} \times \frac{100}{w} \quad (1)$$

where ΔH is the experimental heat of the fusion, w is the weight fraction of the stabilized PLA matrix, and $\Delta H_{f(100)}$ is the heat of the fusion for the pure PLA crystal with a value of 93 J/g [33].

A thermogravimetric analysis (TGA) was used to investigate the relationship between the weight loss and the temperature of the composites. It was performed by thermogravimetry (TA Instruments, model TGA550) in a nitrogen atmosphere with a heating rate of 10 °C/min using a specimen of 3–5 g. The range of the temperature was 50–500 °C.

3.3.6. Water Absorption Testing

The effect of the CFW content on the water absorption of the composites was determined by testing according to ASTM D570-1998. The testing procedure began by preparing a specimen with a size of 50.8 mm in diameter and 3.2 mm in thickness, drying it in the oven at 50 °C for 24 h, and placing it in a container of distilled water maintained at a temperature of 23 °C for 24 h. Afterward, the water on the surface of the specimen was rapidly wiped off with a dry cloth. The specimen was weighed immediately after the water

immersion. The water-absorbing ability was calculated by the difference in the weight before and after the immersion and shown as a percentage.

4. Conclusions

The objective of this work was to study the preparation and characterization of green composites from PLA and cotton fabric waste (CFW) by considering the effect of the CFW content on the composites. The procedure of work began by determining the CFW characteristics to control the quality using a pelletizing technique. The CFW pellets were prepared using compression molding and die-cutting techniques and then compounded with PLA in a twin-screw extruder to form the composite pellets. The testing specimens were produced by compression molding. The results were as follows:

- The melt flow testing showed that an increase in the CFW contents caused the melt flow rate of the composites to decrease.
- The mechanical testing showed that CFW could improve the tensile modulus, flexural strength, and Izod impact strength of PLA. The above mechanical properties of the composites also increased with an increase in the CFW content.
- A fracture morphology observation of the composites showed that an increase in the CFW content caused greater phase separation and roughness on the fracture surface area.
- Thermal property testing, in terms of DSC, showed that an increase in the CFW content caused the T_g and T_m of the composites to slightly increase; the highest were 66.31 °C and 153.54 °C, respectively. The crystallinity increased by approximately 36% compared with pure PLA, but an increase in the CFW content did not clearly change the results. The DSC thermograms of the composites showed one peak, indicating an immiscible blend of PLA and CFW. This could imply that the finishing and dyeing agents that may remain in CFW did not affect the melting point of the composite. In terms of the TGA, the result showed the decomposition of the composites to be lower than pure PLA. The temperature of both the T_{onset} and T_{peak} of the composites decreased with an increase in the CFW content. The decomposition of the composites was shown in a range of 302.41 to 361.22 °C.
- Water absorption testing showed that an increase in the CFW content resulted in the composites having greater water absorption; the highest was 8.76% when compared with pure PLA.
- Based on these results, we expected the green composite based on PLA/CFW can produce the household products such as home decorations and food trays, etc. Moreover, if we can improve the compatibility or toughness of PLA/CFW, it will make more options for manufacturing products.

Author Contributions: Conceptualization, E.J., N.O.-C. and N.P.; methodology, E.J., N.O.-C. and N.P.; validation, E.J. and N.O.-C.; formal analysis, E.J. and N.O.-C.; investigation, N.O.-C.; resources, P.K. and K.C.; data curation, E.J. and N.O.-C.; writing—original draft preparation, E.J. and N.O.-C.; writing—review and editing, E.J. and N.O.-C.; visualization, N.P.; supervision, E.J.; project administration, E.J.; funding acquisition, E.J. and N.P. All authors have read and agreed to the published version of the manuscript.

Funding: This research was funded by Srinakharinwirot University, grant number 550/2564.

Data Availability Statement: The data presented in this study are available on request from the corresponding author.

Acknowledgments: The authors greatly thank Natthapon Apichatsopit and Rattachai Kunthu for their helpful assistance during this project.

Conflicts of Interest: The authors declare no conflict of interest.

References

1. Zhou, Y.; Lei, L.; Yang, B.; Li, J.; Ren, J. Preparation and characterization of polylactic acid (PLA) carbon nanotube nanocomposites. *Polym. Test.* **2018**, *68*, 34–38. [[CrossRef](#)]
2. Zhou, X.; Deng, J.; Fang, C.; Lei, W.; Song, Y.; Zhang, Z.; Huang, Z.; Li, Y. Additive manufacturing of CNTs/PLA composites and the correlation between microstructure and functional properties. *J. Mater. Sci. Technol.* **2021**, *60*, 27–34. [[CrossRef](#)]
3. Park, S.H.; Lee, S.G.; Kim, S.H. Isothermal crystallization behavior and mechanical properties of polylactide/carbon nanotube nanocomposites. *Compos. Part A Appl. Sci. Manuf.* **2013**, *46*, 11–18. [[CrossRef](#)]
4. Kaseem, M.; Hamad, K.; Ur Rehman, Z. Review of recent advances in polylactic acid/TiO₂ composites. *Materials* **2019**, *12*, 3659. [[CrossRef](#)]
5. Buzarovska, A.; Grozdanov, A. Biodegradable poly (L-lactic acid)/TiO₂ nanocomposites: Thermal properties and degradation. *J. Appl. Polym. Sci.* **2012**, *123*, 2187–2193. [[CrossRef](#)]
6. Zhuang, W.; Liu, J.; Zhang, J.H.; Hu, B.X.; Shen, J. Preparation, characterization, and properties of TiO₂/PLA nanocomposites by in situ polymerization. *Polym. Compos.* **2009**, *30*, 1074–1080. [[CrossRef](#)]
7. Huda, M.S.; Drzal, L.T.; Mohanty, A.K.; Misra, M. Chopped glass and recycled newspaper as reinforcement fibers in injection molded poly (lactic acid)(PLA) composites: A comparative study. *Compos. Sci. Technol.* **2006**, *66*, 1813–1824. [[CrossRef](#)]
8. Siakeng, R.; Jawaid, M.; Ariffin, H.; Sapuan, S.; Asim, M.; Saba, N. Natural fiber reinforced polylactic acid composites: A review. *Polym. Compos.* **2019**, *40*, 446–463. [[CrossRef](#)]
9. Wang, N.; Zhang, X.; Ma, X.; Fang, J. Influence of carbon black on the properties of plasticized poly (lactic acid) composites. *Polym. Degrad. Stab.* **2008**, *93*, 1044–1052. [[CrossRef](#)]
10. Muller, J.; González-Martínez, C.; Chiralt, A. Combination of poly (lactic acid) and starch for biodegradable food packaging. *Materials* **2017**, *10*, 952. [[CrossRef](#)] [[PubMed](#)]
11. Sun, X.S. Plastics derived from starch and poly. In *Bio-Based Polymers and Composites*; Academic Press: Cambridge, MA, USA, 2005; p. 369.
12. Zini, E.; Scandola, M. Green composites: An overview. *Polym. Compos.* **2011**, *32*, 1905–1915. [[CrossRef](#)]
13. La Mantia, F.; Morreale, M. Green composites: A brief review. *Compos. Part A Appl. Sci. Manuf.* **2011**, *42*, 579–588. [[CrossRef](#)]
14. Bajpai, S.; Mary, G.; Chand, N. The use of cotton fibers as reinforcements in composites. In *Biofiber Reinforcements in Composite Materials*; Elsevier: Amsterdam, The Netherlands, 2015; pp. 320–341.
15. Juanga-Labayen, J.P.; Labayen, I.V.; Yuan, Q. A review on textile recycling practices and challenges. *Textiles* **2022**, *2*, 174–188. [[CrossRef](#)]
16. Mwaikambo, L.Y.; Ansell, M.P. Chemical modification of hemp, sisal, jute, and kapok fibers by alkalization. *J. Appl. Polym. Sci.* **2002**, *84*, 2222–2234. [[CrossRef](#)]
17. Aziz, S.H.; Ansell, M.P. The effect of alkalization and fibre alignment on the mechanical and thermal properties of kenaf and hemp bast fibre composites: Part 1—Polyester resin matrix. *Compos. Sci. Technol.* **2004**, *64*, 1219–1230. [[CrossRef](#)]
18. Sanivada, U.K.; Mármol, G.; Brito, F.; Fangueiro, R. PLA composites reinforced with flax and jute fibers—A review of recent trends, processing parameters and mechanical properties. *Polymers* **2020**, *12*, 2373. [[CrossRef](#)]
19. Kamarudin, S.H.; Abdullah, L.C.; Aung, M.M.; Ratnam, C.T. Mechanical and physical properties of Kenaf-reinforced Poly (lactic acid) plasticized with epoxidized Jatropa Oil. *BioResources* **2019**, *14*, 9001–9020.
20. Tawakkal, I.S.M.; Talib, R.A.; Abdan, K.; Ling, C.N. Mechanical and physical properties of kenaf-derived cellulose (KDC)-filled polylactic acid (PLA) composites. *BioResources* **2012**, *7*, 1643–1655. [[CrossRef](#)]
21. Bajracharya, R.M.; Bajwa, D.S.; Bajwa, S.G. Mechanical properties of polylactic acid composites reinforced with cotton gin waste and flax fibers. *Procedia Eng.* **2017**, *200*, 370–376. [[CrossRef](#)]
22. Piekarska, K.; Piorowska, E.; Krasnikova, N.; Kulpinski, P. Polylactide composites with waste cotton fibers: Thermal and mechanical properties. *Polym. Compos.* **2014**, *35*, 747–751. [[CrossRef](#)]
23. Zhang, X.; Shen, J.; Yang, T.; Ye, B.; Lin, Z.; Tan, S. Characteristics of poly(lactic acid) reinforced composites with waste cotton. *J. Polym. Eng.* **2011**, *31*, 531–537. [[CrossRef](#)]
24. Qian, J.; Yu, M.M.; Ge, Z.; Xu, M.J.; Zhang, H.H.; Yang, G.S.; Shao, H.L. Preparation and properties of cotton fiber/poly (lactic acid) composites. *Mater. Sci. Forum* **2014**, *789*, 100–105. [[CrossRef](#)]
25. Siddika, S.; Mansura, F.; Hasan, M. Physico-mechanical properties of jute-coir fiber reinforced hybrid polypropylene composites. *Eng. Technol.* **2013**, *73*, 1145–1149.
26. Rahman, M.; Mondol, M.; Hasan, M. Mechanical properties of chemically treated coir and betel nut fiber reinforced hybrid polypropylene composites. In *Proceedings of the IOP Conference Series: Materials Science and Engineering*, Dhaka, Bangladesh, 1–3 March 2018; p. 012025.
27. McKeen, L.W. *The Effect of Sterilization on Plastics and Elastomers*, 3rd ed.; William Andrew: Oxford, UK, 2012; pp. 57–84.
28. Richards, R. Polyethylene—Structure, crystallinity and properties. *J. Appl. Chem.* **1951**, *1*, 370–376. [[CrossRef](#)]
29. Tserki, V.; Matzinos, P.; Panayiotou, C. Effect of compatibilization on the performance of biodegradable composites using cotton fiber waste as filler. *J. Appl. Polym. Sci.* **2003**, *88*, 1825–1835. [[CrossRef](#)]
30. Ceylan, Ö.; Van Landuyt, L.; Rahier, H.; De Clerck, K. The effect of water immersion on the thermal degradation of cotton fibers. *Cellulose* **2013**, *20*, 1603–1612. [[CrossRef](#)]

31. Shahedifar, V.; Rezadoust, A.M. Thermal and mechanical behavior of cotton/vinyl ester composites: Effects of some flame retardants and fiber treatment. *J. Reinf. Plast. Compos.* **2013**, *32*, 681–688. [[CrossRef](#)]
32. Jansri, E.; Narongchai, O. Polypropylene/polyethylene two-layered by one-step rotational molding. *J. Polym. Eng.* **2018**, *38*, 685–694. [[CrossRef](#)]
33. Farah, S.; Anderson, D.G.; Langer, R. Physical and mechanical properties of PLA, and their functions in widespread applications—A comprehensive review. *Adv. Drug Deliv. Rev.* **2016**, *107*, 367–392. [[CrossRef](#)]